



Article

Effects of Deacetylase Inhibition on the Activation of the Antioxidant Response and Aerobic Metabolism in Cellular Models of Fanconi Anemia

Nadia Bertola ¹, Stefano Regis ², Silvia Bruno ¹, Andrea Nicola Mazzarello ¹, Martina Serra ², Michela Lupia ³, Federica Sabatini ⁴, Fabio Corsolini ⁵, Silvia Ravera ^{1,*} and Enrico Cappelli ^{3,†}

¹ Department of Experimental Medicine, University of Genoa, Via De Toni 14, 16132 Genoa, Italy

² Laboratory of Clinical and Experimental Immunology, IRCCS Istituto Giannina Gaslini, Via Gerolamo Gaslini 5, 16148 Genova, Italy

³ Haematology Unit, IRCCS Istituto Giannina Gaslini, Via Gerolamo Gaslini 5, 16148 Genova, Italy

⁴ Stem Cell Laboratory and Cell Therapy Center, IRCCS Istituto Giannina Gaslini, Via Gerolamo Gaslini 5, 16148 Genova, Italy

⁵ Centro di Diagnostica Genetica e Biochimica delle Malattie Metaboliche, IRCCS Istituto Giannina Gaslini, Via Gerolamo Gaslini 5, 16148 Genova, Italy

* Correspondence: silvia.ravera@unige.it

† These authors contributed equally to this work.



Citation: Bertola, N.; Regis, S.; Bruno, S.; Mazzarello, A.N.; Serra, M.; Lupia, M.; Sabatini, F.; Corsolini, F.; Ravera, S.; Cappelli, E. Effects of Deacetylase Inhibition on the Activation of the Antioxidant Response and Aerobic Metabolism in Cellular Models of Fanconi Anemia. *Antioxidants* **2023**, *12*, 1100. <https://doi.org/10.3390/antiox12051100>

Academic Editor: Alessandro Allegra

Received: 13 February 2023

Revised: 6 May 2023

Accepted: 12 May 2023

Published: 15 May 2023

Correction Statement: This article has been republished with a minor change. The change does not affect the scientific content of the article and further details are available within the backmatter of the website version of this article.



Copyright: © 2023 by the authors. Licensee MDPI, Basel, Switzerland. This article is an open access article distributed under the terms and conditions of the Creative Commons Attribution (CC BY) license (<https://creativecommons.org/licenses/by/4.0/>).

Abstract: Fanconi anemia (FA) is a rare genetic disease characterized by a dysfunctional DNA repair and an oxidative stress accumulation due to defective mitochondrial energy metabolism, not counteracted by endogenous antioxidant defenses, which appear down-expressed compared to the control. Since the antioxidant response lack could depend on the hypoacetylation of genes coding for detoxifying enzymes, we treated lymphoblasts and fibroblasts mutated for the *FANCA* gene with some histone deacetylase inhibitors (HDACi), namely, valproic acid (VPA), beta-hydroxybutyrate (OHB), and EX527 (a Sirt1 inhibitor), under basal conditions and after hydrogen peroxide addition. The results show that VPA increased catalase and glutathione reductase expression and activity, corrected the metabolic defect, lowered lipid peroxidation, restored the mitochondrial fusion and fission balance, and improved mitomycin survival. In contrast, OHB, despite a slight increase in antioxidant enzyme expressions, exacerbated the metabolic defect, increasing oxidative stress production, probably because it also acts as an oxidative phosphorylation metabolite, while EX527 showed no effect. In conclusion, the data suggest that VPA could be a promising drug to modulate the gene expression in FA cells, confirming that the antioxidant response modulation plays a pivotal in FA pathogenesis as it acts on both oxidative stress levels and the mitochondrial metabolism and dynamics quality.

Keywords: catalase; glutathione reductase; oxidative phosphorylation; lipid peroxidation; aldehyde dehydrogenase; energy metabolism; antioxidant defenses; histone deacetylase inhibitors

1. Introduction

Fanconi anemia is a genomic instability syndrome mainly characterized by bone marrow failure [1,2] and cancer predisposition [3–5] due to an impairment in DNA inter-strand crosslink (ICLs) repair [6,7]. In addition, FA cells show dysfunctional oxidative phosphorylation (OxPhos) [8–10] caused by an altered electron transport between respiratory complexes I and III [11–13]. Because of the aerobic metabolism impairment, FA cells show a metabolic switch toward lactate fermentation [14] and acetyl-CoA accumulation that causes an increase in fatty acid synthesis and lipid droplet accumulation [15]. The dysfunctional mitochondrial metabolism in FA cells is also associated with high oxidative stress production [9,16,17], which represents one of the causes of ICLs [18]. In addition, FA cells appear unable to counteract the oxidative stress increment since the expression and

the activity of endogenous antioxidant defenses, such as catalase, glutathione reductase, glutathione peroxidase, and aldehyde dehydrogenase, is lower than in healthy cells and does not increase after oxidative stress insult [13,17].

Gene expression is regulated by different chromatin modifications [19], including acetylation, which plays a pivotal role in transcriptional regulation as it modulates the chromatin accessibility of transcriptional and DNA repair proteins [20]. The acetylation status depends on the balance between the deacetylase (HDAC) and acetyltransferase (HAT) enzymatic activity [21]. While histone acetylation leads to increased gene expression, deacetylation has the opposite effect. Moreover, acetylation represents a fundamental post-translational modification that determines different proteins' functions or localization [22]. So far, there are 18 HDAC enzymes subdivided into four classes [23,24]. Classes I, II, and IV are zinc dependent, and III is NAD⁺ dependent [23]. Histone deacetylase inhibitors (HDACi) modify gene expression at many levels [25] and are used in several diseases, such as chronic inflammatory disorders [26–30], cancers [31–34], and neurodegenerative diseases [35,36].

The role of chromatin modifications in FA cells remains slightly investigated. Renaud et al. show that chromatin in FA cells is hypoacetylated, allowing the localization of 53BP1, a mammalian non-homologous DNA end-joining (NHEJ) protein, on DNA double-strand breaks (DSB) [37]. Treatment with an HDACi counteracts the cytotoxic effect of NHEJ, preventing the localization of 53BP1 protein on DNA DSB and leaving free access to the homologous recombination protein [38,39].

Thus, this work investigated the HDACi effects on antioxidant response and energy metabolism in lymphoblasts and fibroblasts carrying the mutation for the *FANCA* gene. In particular, FA lymphoblasts and fibroblasts were treated with three different HDACi: valproic acids (VPA), beta-hydroxybutyrate (OHB), and EX527.

Our results show that VPA and, to a lesser extent, OHB induce the expression and activity of catalase and glutathione reductase, enzymes involved in the antioxidant response in FA cells. However, only VPA improves mitochondrial metabolism, reducing oxidative stress and MMC sensibility. Conversely, OHB causes a loss of OxPhos efficiency and increases the accumulation of lipid droplets and malondialdehyde, whereas EX527 does not affect energy metabolism and antioxidant defense activity.

2. Materials and Methods

2.1. Materials

All chemical compounds were of the highest chemical grade and were purchased from Sigma-Aldrich (St. Louis, MO, USA).

2.2. HDACi Treatment

To inhibit histone deacetylases (HDAC), three different molecules were employed: valproic acid (VPA), beta-hydroxybutyrate (OHB), and EX527. In detail, VPA is a drug used for seizures and bipolar disorder [40], which inhibits class I (HDAC1, 2, 3, and 8) and class IIa (HDAC4, 5, 7, and 9) [41], providing an anti-cancer effect [42]. The ketone body OHB is a specific class I HDACi (HDAC1 and HDAC2) that promotes the transcription of catalase and mitochondria super-oxide dismutase genes by increasing the expression of FoxO3A and MT2 genes, two oxidative stress resistance factors [43]. EX527 is a specific inhibitor of sirtuin 1 (SIRT1) and, to a lesser extent, sirtuin 6 (SIRT6) [44,45], two HDAC belonging to class III deacetylases regulating the response to stress and mitochondrial biogenesis [46].

In this manuscript, both lymphoblast and fibroblast cell lines were treated with 1 mM VPA [47], 10 mM OHB [43,48], or 100 nM EX257 [44]. Drugs' effects on antioxidant defenses and aerobic metabolism were investigated 3 or 24 h after the treatment. Specifically, at the 3 h time point, the effects of short-term HDACi treatment on the expression and activity of antioxidant enzymes were evaluated; experiments after 24 h from the treatment were performed to assess whether the antioxidant defense restoration could promote and improve oxidative metabolism.

2.3. Cell Culture

Six different *FANC-A* lymphoblast cell lines (Lympho FA) and three different *FANC-A* primary fibroblast cell lines (Fibro FA) derived from six patients who carried out different mutations of the *FANC-A* gene were obtained from the “Cell Line and DNA Biobank from Patients affected by Genetic Diseases” (G. Gaslini Institute)—Telethon Genetic Biobank Network (Project No. GTB07001). As controls, isogenic FA-corr cell lines generated by the same *FANC-A* lymphoblast and fibroblast cell lines corrected with S11FAIN retrovirus (Lympho FA-corr and Fibro FA-corr) were employed [12,49]. In addition, lymphoblast cell lines and primary fibroblasts isolated from healthy donors were also employed to demonstrate that isogenic corrected cells represent a proper control. The data reported in Figures S1 and S2, respectively, showed no difference between healthy and FA-corr cells in the biochemical readouts used in this manuscript.

For lymphoblast cell lines, RPMI-1640 medium (#21875091, GIBCO, Billing, MT, USA) containing 10% FBS (#ECS0120L, Euroclone, Milano, Italy), 100 U/mL penicillin, and 100 µg/mL streptomycin (#ECB3001D, Euroclone, Milano, Italy) was used, and the cells were grown at 37 °C with a 5% CO₂ [12]. Primary fibroblasts were cultured as a monolayer in DMEM high glucose with glutamax[®] (#61965026, GIBCO, Billing, MT, USA), containing 10% fetal bovine serum (FBS; #ECS0120L, Euroclone, Milano, Italy), 100 U/mL penicillin, and 100 µg/mL streptomycin (#ECB3001D, Euroclone, Milano, Italy) at 37 °C with a 5% CO₂.

When necessary, 0.5 mM hydrogen peroxide (H₂O₂) was added to induce oxidative damage.

2.4. Gene Expression Evaluation

RNA was extracted from lymphoblast pellets using the RNeasy mini kit (Qiagen, Hilden, Germany). To evaluate the expression of catalase (*CAT*) and glutathione reductase (*GR*) mRNAs, 100 ng of RNA was reverse-transcribed using the SuperScript VILO IV cDNA Synthesis Kit (Invitrogen, Waltham, MA, USA). Real-time PCR was performed on the cDNA using the primers-probe mix contained in the specific TaqMan Gene Expression Assays (Applied Biosystems, Waltham, MA, USA). Gene expression was normalized to the *GAPDH* expression. Experiments were performed in triplicate.

2.5. Cell Homogenate Preparation and Treatment

After two washes in PBS, primary fibroblasts and lymphoblasts pellets were resuspended in PBS supplied with protease inhibitors (P2714, Sigma-Aldrich, St. Louis, MO, USA) and sonicated (Microson XL Model DU-2000, Misonix Inc., Farmingdale, NY, USA) twice for 10 s, with a 30 s break and in ice to prevent heating. Total protein content was assayed by the Bradford method [50].

2.6. Antioxidant Enzyme Activity Evaluation

Catalase (*CAT*), glutathione reductase (*GR*), and aldehyde dehydrogenase (*ALDH*) were assayed as markers of cellular antioxidant defenses. For each assay, 50 µg of total proteins was used.

CAT activity was assayed spectrophotometrically following the H₂O₂ decomposition at 240 nm. The assay mix contained 50 mM phosphate buffer (pH 7.0) and 5 mM H₂O₂ [51].

GR activity was assayed spectrophotometrically at 340 nm, following the NADPH oxidation. The assay medium contained 100 mM Tris-HCl (pH 7.4), 1 mM EDTA, 5 mM GSSG, and 0.2 mM NADPH [52].

ALDH activity was measured spectrophotometrically at 340 nm following the NAD⁺ oxidation. The assay mix contained 100 mM sodium pyrophosphate (#221368 Sigma-Aldrich, St. Louis, MO, USA) at pH 9, 10 mM NAD⁺ (N0632 Sigma-Aldrich, St. Louis, MO, USA), and 10 mM acetaldehyde (#402788 Sigma-Aldrich, St. Louis, MO, USA) [53].

2.7. Lipid Peroxidation Evaluation

Lipid peroxidation damage was evaluated spectrophotometrically at 532 nm by the malondialdehyde (MDA) concentration assay, using the thiobarbituric acid reactive substance (TBARS) assay. For each sample, 50 µg of total protein was dissolved in 300 µL of Milli-Q water and 600 µL of TBARS solution [54].

2.8. Lipid Content Evaluation

The lipid content was evaluated spectrophotometrically at 535 nm by the Sulfo-Phospho-Vanillin assay, according to [13]. A mix of triglycerides (#17810, Sigma-Aldrich, St. Louis, MO, USA) was employed for the standard curve.

2.9. Evaluation of Electron Transport between Complexes I and III

The electron transfer between complex I and complex III was assayed spectrophotometrically at 550 nm following the reduction of cytochrome c on 50 µg of total protein. The reaction mix contained 100 mM Tris-HCl (pH 7.4), 0.03% of oxidized cytochrome c (#C2867, Sigma-Aldrich, St. Louis, MO, USA), and 0.7 mM NADH [55].

2.10. ATP and AMP Intracellular Content Evaluation

For each assay, 50 µg of total protein was used.

ATP was assayed spectrophotometrically following NADP reduction at 340 nm. Assay medium contained 100 mM Tris-HCl (pH 8.0), 0.2 mM NADP, 5 mM MgCl₂, and 50 mM glucose. Samples were analyzed before and after the addition of 3 µg of purified hexokinase plus glucose-6-phosphate dehydrogenase [56].

AMP was assayed spectrophotometrically following NADH oxidation at 340 nm. Reaction medium contained 100 mM Tris-HCl (pH 8.0), 5 mM MgCl₂, 0.2 mM ATP, 10 mM phosphoenolpyruvate, 0.15 mM NADH, 10 IU adenylate kinase, 25 IU pyruvate kinase, and 15 IU lactate dehydrogenase [56].

The ratio between the intracellular concentrations of ATP and AMP (ATP/AMP) represents a marker of cellular energy status.

2.11. Oxidative Phosphorylation Evaluation

Oxidative phosphorylation (OxPhos) metabolism was evaluated as oxygen consumption rate (OCR) and ATP synthesis through FoF1 ATP-synthase. For each assay, 105 cells, permeabilized with 0.03 mg/mL digitonin for 1 min, were employed. In both cases, 10 mM pyruvate plus 5 mM malate (#P4562 and #M8304, respectively, Sigma-Aldrich, St. Louis, MO, USA) or 20 mM succinate (#S7501, Sigma-Aldrich, St. Louis, MO, USA) was used as a respiratory substrate to stimulate the respiratory pathway led by Complex I or by Complex II, respectively.

OCR was measured with an amperometric electrode (Unisense Microrespiration, Unisense A/S, Aarhus, Denmark) [14,57].

ATP synthesis was monitored with a luminometer (GloMax[®] 20/20 Luminometer, Promega Italia, Milano, Italy) by the luciferin/luciferase chemiluminescent method (luciferin/luciferase ATP bioluminescence assay kit CLS II, Roche, Basilea, Switzerland) for 2 min every 30 s. ATP standard solutions in a concentration range between 10⁻⁸ and 10⁻⁵ M were used for the calibration curve [14,57].

2.12. Mitochondrial Energy Metabolism Efficiency Calculation

To evaluate the OxPhos efficiency, the ratio between the aerobic synthesized ATP and the consumed oxygen (P/O) was calculated. Efficient mitochondria displayed a P/O value of around 2.5 or 1.5 when stimulated with pyruvate and malate or succinate, respectively. A P/O ratio lower than these values indicates that oxygen is not completely devoted to energy production but contributes to reactive oxygen species (ROS) formation [58].

2.13. Confocal Microscopy Analysis

Cells were cultured in chamber slides for 24 h in the absence or presence of the three HDACi. After fixation with 0.3% paraformaldehyde (#P6148, Sigma-Aldrich, St. Louis, MO, USA) and permeabilization with 0.1% triton (#X100, Sigma-Aldrich, St. Louis, MO, USA), cells were incubated with anti-TOM20 antibody (#42406S, Cell Signaling Technology, Danvers, MA, USA) overnight at 4 °C. Afterward, cells were incubated for 1 h at 25 °C with the Alexa-546-conjugated anti-rabbit antiserum (#A11010, Invitrogen, USA) as a secondary antibody.

Immunofluorescence confocal laser scanner microscopy (CLSM) imaging was carried out using a laser scanning spectral confocal microscope TCS SP2 AOBS (Leica, Germany), equipped with Argon ion, He–Ne 543 nm, and He–Ne 633 nm lasers. Images were acquired through an HCX PL APO CS 40×/1.25 oil UV objective and processed with Leica. Images were acquired as single transcellular optical sections.

To evaluate the mitochondrial network shape, fibroblasts were scored depending on the morphology of most of their mitochondrial population as elongated or intermediated/short following the method described in [59].

2.14. Western Blot Analysis

After denaturing electrophoresis (SDS-PAGE), nitrocellulose membrane was incubated with anti-MFN2 (#11925S, Cell Signaling Technology, Danvers, MA, USA), anti-DRP1 (#ab184247, Abcam, Cambridge, UK), anti-UCP2 (#sc-6525, Santa Cruz Biotechnology, Dallas, TX, USA), and anti-Actin (#sc-1616, Santa Cruz Biotechnology, Dallas, TX, USA). All primary antibodies were diluted in PBS plus 0.15% Tween (PBSt, Tween was from Roche, Basilea, Switzerland, #11332465001). Secondary antibodies (#A0168 and #SAB3700870, Sigma-Aldrich, St. Louis, MO, USA) were diluted 1:10,000 in PBSt. Bands were evaluated by a chemiluminescence system (Alliance 6.7 WL 20M, UVITEC., Cambridge, UK) using an enhanced chemiluminescence substrate (ECL, #1705061, BioRad, Hercules, CA, USA). Band intensity was evaluated by Alliance™ Q9-Series software (UVITEC, Cambridge, UK). All the signals were normalized versus the actin signal.

2.15. Mitomycin C Survival Assay

Lymphoblast cell line survival under mitomycin C (MMC) treatment (0, 1, 3, 10, and 33 nM) was tested as previously described in Bottega et al. [60].

2.16. Statistical Analysis

Data were analyzed by one-way ANOVA followed by Tukey's multiple comparison test by Prism 8 Software. Data are expressed as mean ± standard deviation (SD) and are representative of 6 independent experiments. Errors with a probability of $p < 0.05$ were considered significant.

3. Results

3.1. VPA and OHB Treatment Enhanced Catalase and Glutathione Reductase Expression and Activity in Cells Mutated for the FANC-A Gene

Figure 1 shows that expression and activity of CAT (Panels A and C) and GR (Panels B and D), two enzymes involved in cellular antioxidant responses, were low in lymphoblasts mutated for the FANC-A gene with respect to the FA-corr cells, confirming the inability of FA cells to counteract the oxidative stress production by enhancing the antioxidant defenses [13].

Thus, to improve the expression and activity of enzymes involved in oxidative stress detoxification, FA cells were treated with VPA, OHB, or EX527, three histone deacetylase inhibitors [41,43,45]. The results show that, already after 3 h of treatment, VPA caused an enhancement in CAT and GR expression and activity in FA lymphoblasts, which was even more evident 24 h after the addition of the drug (Figure 1A,C). CAT and GR expression and activity also increased with OHB, but only after 24 h of treatment (Figure 1B,D). However, the drug-induced improvement did not reach the FA-corr cell level in both cases.

By contrast, treatment with EX527 did not affect the expression and activity of the two enzymes (Figure 1). The same results on enzymatic activity were observed in primary fibroblasts (Figure S3).

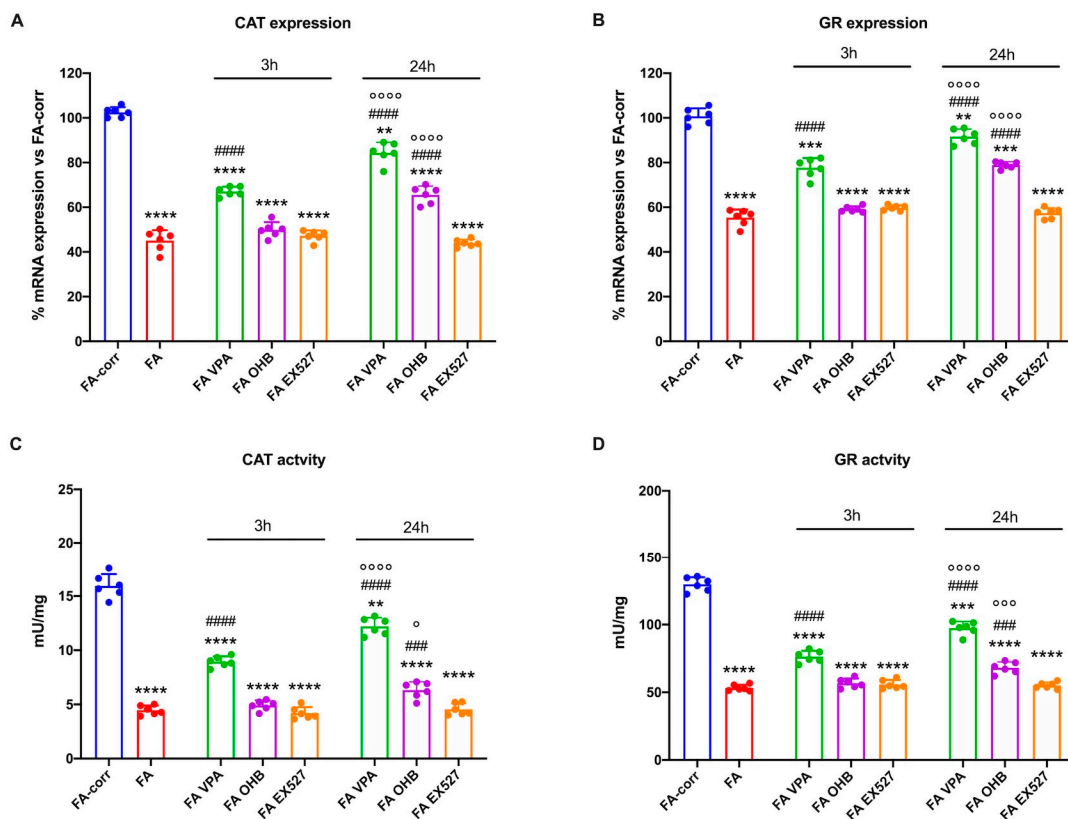


Figure 1. Modulation of catalase and glutathione reductase expression and activity in FA lymphoblasts treated with VPA, OHB, or EX527. (A) Catalase (CAT) gene expression; (B) glutathione reductase (GR) gene expression; (C) CAT activity; (D) GR activity. In each panel, the effects were evaluated in lymphoblasts after 3 and 24 h from VPA, OHB, or EX527 addition. Data are reported as mean \pm SD, and each graph is representative of 6 independent experiments. Statistical significance was tested with a one-way ANOVA. **, ***, and **** represent a significant difference for $p < 0.01$, 0.001, or 0.0001, respectively, between FA and FA-corr cells used as control. ### and #### represent a significant difference for $p < 0.001$ or 0.0001, respectively, between untreated and treated FA cells. \circ , $\circ\circ$, and $\circ\circ\circ$ represent a significant difference for $p < 0.05$, 0.001, or 0.0001, respectively, between the same treatment at 3 and 24 h.

3.2. VPA but Not OHB and EX527 Improved the lipid Profile and Mitochondrial Energy Metabolism in Cells Carrying the FANC-A Mutation

The unfunctional antioxidant response exacerbated the metabolic alteration of FA cells, as a vicious circle was created between uncontrolled oxidative stress production and mitochondrial metabolic dysfunction [61,62]. Thus, several metabolic markers were evaluated after 24 h of treatment on lymphoblast cell lines (Figure 2) and primary fibroblasts (Figure S4) to investigate whether increased antioxidant enzyme activity also improved the energy metabolism defect.

The VPA addition enhanced OCR and ATP synthesis (Figures 2A,B and S4A,B), although FA-corr cell values were not achieved. The aerobic metabolism amelioration improved the OxPhos efficiency, as suggested by the recovery of P/O ratio values in the presence of pyruvate/malate (Figures 2C and S4C) thanks to the enhancement of the electron transfer between respiratory complexes I and III (Figures 2D and S4D). The mitochondrial function recovery caused, in turn, an improvement of cellular energy status, as

shown by the increase in the ATP/AMP ratio (Figures 2E and S4E) and a reduction in lipid content (Figures 2F and S4F), as better functioning OxPhos does not determine acetyl-CoA accumulation and its conversion in fatty acids.

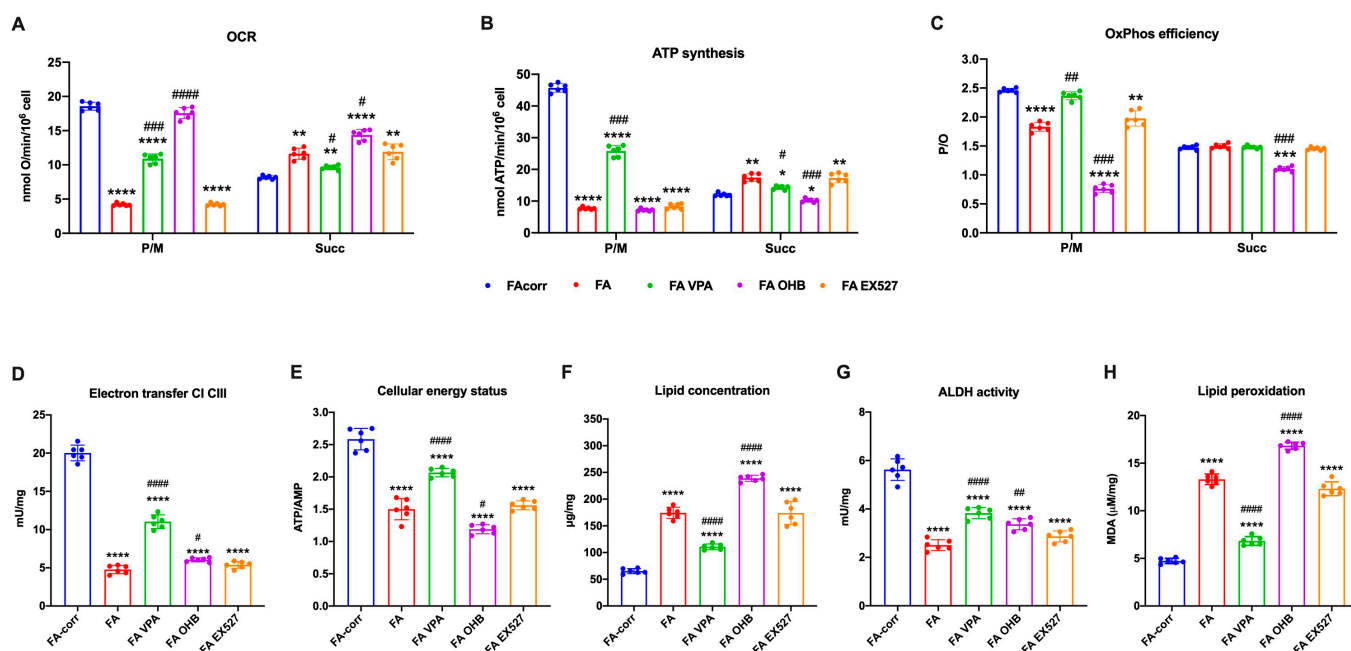


Figure 2. VPA, OHB, and EX527 effects on energy metabolism parameters and lipid peroxidation in FA lymphoblasts. (A) Oxygen Consumption Rate (OCR); (B) ATP synthesis through F₀F₁ ATP synthase; (C) P/O ratio as an OxPhos efficiency marker. For Panels A–C, pyruvate/malate (P/M) and succinate (Succ) were employed as respiratory substrates. (D) Electron transfer between complexes I and III; (E) ATP/AMP ratio as a cellular energy status marker; (F) cellular lipid concentration; (G) aldehyde dehydrogenase (ALDH) activity; (H) malondialdehyde (MDA) intracellular concentration as a lipid peroxidation marker. In each panel, the effects were evaluated in lymphoblasts after 24 h from the VPA, OHB, or EX527 addition. Data are reported as mean ± SD, and each graph is representative of 6 independent experiments. Statistical significance was tested opportunely with a one-way ANOVA. *, **, ***, and **** represent a significant difference for *p* < 0.05, 0.01, 0.001, or 0.0001, respectively, between FA and FA-corr cells used as control. #, ##, ###, and #### represent a significant difference for *p* < 0.05, 0.01, 0.001, or 0.0001, respectively, between untreated and treated FA cells.

In addition, VPA increased the ALDH activity, an enzyme involved in aldehydes detoxification (Figures 2G and S4G). The oxidative stress detoxification improvement and reduced intracellular lipid concentration could explain the decrease in lipid peroxidation (Figures 2H and S4H).

By contrast, OHB treatment caused an increase in the uncoupling between oxygen consumption and energy production, as suggested by the OCR increment and the ATP synthesis decrease in the presence of both respiratory substrates (Figures 2A,B and S4A,B), further reducing both P/O ratio values compared to untreated FA cells (Figures 2C and S4C). Therefore, despite a slight electron transfer increment between complexes I and III (Figures 2D and S4D), the cellular energy state did not improve (Figures 2E and S4E), and the unfunctional OxPhos increased the lipid content (Figures 2F and S4F). Furthermore, OHB did not affect the activity of ALDH (Figures 2G and S4G), nor those of CAT and GR, causing an accumulation of lipid peroxidation (Figures 2H and S4H), as the uncoupling of OxPhos is not counteracted by antioxidant defenses.

No effects on the metabolic parameters were observed for EX527 treatment (Figures 2 and S4).

Interestingly, positive effects of VPA treatment on biochemical parameters were also seen in the ability of FA lymphoblasts to survive MMC (Figure 3).

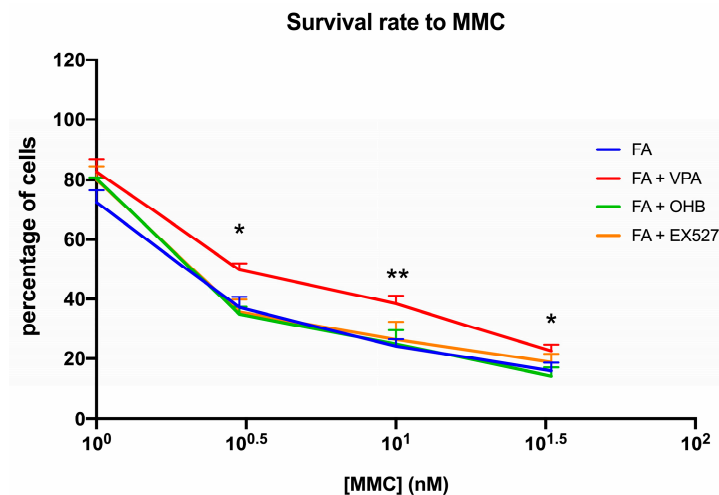


Figure 3. VPA, OHB, or EX527 treatment effect on mitomycin survival. The graph shows the mitomycin (MMC) survival rate of FA lymphoblasts treated with VPA, OHB, or EX527. Data are reported as mean \pm SD, and each graph is representative of 6 independent experiments. Statistical significance was tested with a one-way ANOVA. * and ** represent a significant difference for $p < 0.05$ or 0.01 , respectively, between FA and FA-corr cells used as control.

3.3. VPA Treatment Improved the Balance between Fusion and Fission and Reduced the UCP2 Expression, Recovering the Mitochondrial Network Shape

FA cells are characterized by a disrupted mitochondrial network [63], in which organelles appear swollen with less defined cristae [12,63,64]. These structural alterations could be associated with unbalanced mitochondrial dynamics, as suggested by the WB analyses (Figure 4A,B). In particular, FA fibroblasts express a high level of DRP1, a protein involved in mitochondrial fission, compared to the control. Conversely, levels of MFN2, a protein involved in fusion, are similarly expressed in FA-corr and FA cells, causing an unbalanced in the mitochondrial network organization towards the fission as confirmed by the confocal images (Figure 4C). In addition, also the uncoupling protein 2 (UCP2) was found to be overexpressed in the FA fibroblast, justifying the low OxPhos efficiency (Figure 4A,B). In addition, Figure 4C shows that FA fibroblasts more often exhibited intermediated/short and less elongated mitochondria compared to FA-corr cells. Interestingly, treatment with VPA recovered DRP1 and UCP2 levels similar to the control cells (Figure 4A,B), restoring the elongated structures and, thus, the mitochondrial network shape organization (Figure 4C).

3.4. FA Cells Were Unable to Counterbalance the Effects of a Pro-Oxidant Event except in the Presence of VPA

Considering that antioxidant defenses increase in response to an oxidative insult, the VPA, OHB, or EX527 effects were evaluated in FA-corr and FA-lymphoblastoid lines treated with hydrogen peroxide.

The results show that FA-corr lymphoblasts increased the expression and activity of CAT and GR already after 3 h of H₂O₂ treatment (Figure 5A,C,E,G), maintaining elevated defenses even 24 h after the oxidative damage (Figure 5B,D,F,H). Furthermore, the observed increase did not improve after the VPA, OHB, or EX527 addition, suggesting that control cells themselves trigger an adaptive response to oxidative stress and that HDCAi are not required to raise defenses.

In contrast, FA lymphoblasts, in the presence of H₂O₂, further decreased low CAT and GR expression and activity, probably due to the accumulation of oxidative damage. However, VPA, even under pro-oxidant conditions, induced CAT and GR expression and activity improvement after 3 h and 24 h of treatment. OHB also caused an enhancement in antioxidant defenses, but only after 24 h of treatment, whereas EX527 showed no effect. Similar results were obtained on primary fibroblasts (Figure S5).

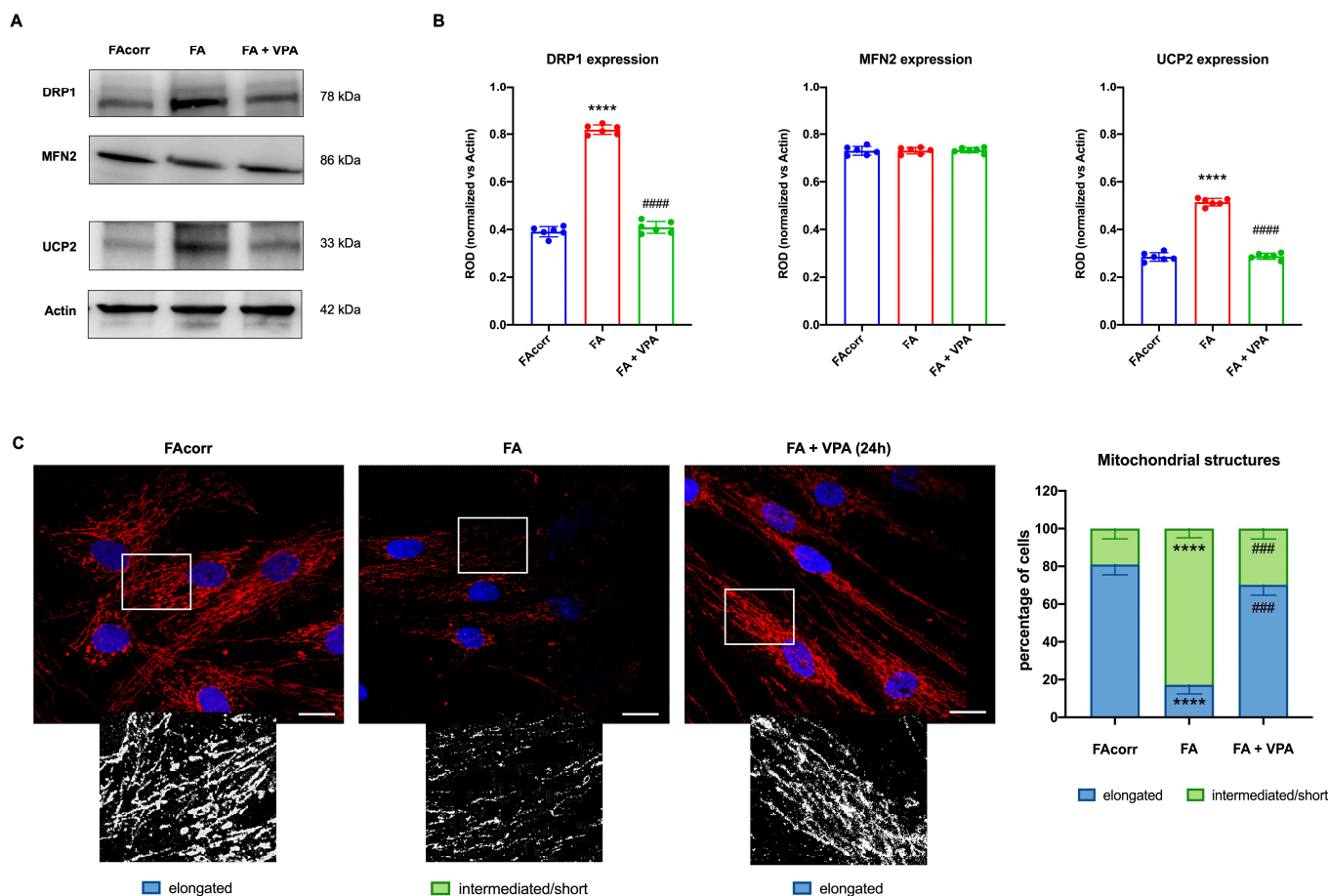


Figure 4. VPA modulation of mitochondrial dynamic and uncoupling protein 2 expression in FA primary fibroblasts. (A) WB signals and (B) relative densitometry of DRP1 (mitochondrial fission), MFN2 (mitochondrial fusion), uncoupling protein 2 (UCP2), and Actin (housekeeping protein used for signal normalization) in FA-corr and FA primary fibroblasts treated or not with VPA for 24 h. Each signal was normalized on the actin signal. (C) Confocal imaging of FA-corr and FA fibroblasts stained with antibody against TOM20 (red) and DAPI (blue) to show the mitochondrial reticulum and nuclei, respectively. White scale bars correspond to 10 μ m. The higher magnification inserts, corresponding to the area enclosed by the white square, represent an example of mitochondrial network distribution. Data reported in the histogram on the right are expressed as mean \pm SD. Each panel is representative of at least 6 independent experiments. Statistical significance was tested with a one-way ANOVA. **** represents a significant difference for $p < 0.0001$ between FA cells and FA-corr. ### and #### represent a significant difference for $p < 0.001$ or 0.0001 , respectively, between untreated and VPA-treated FA fibroblasts.

Regarding energy metabolism, the H₂O₂ addition to FA-corr lymphoblasts did not cause any significant effect (Figure 6), except for a slight decrease in the ATP/AMP ratio, which may depend on increased energy expenditure to counteract oxidative stress. Treatment with VPA, OHB, and EX527 concomitant with the oxidative insult also caused limited changes in FA-corr, in particular, an ATP/AMP ratio recovery, reaching levels similar to those of control cells not treated with H₂O₂. In addition, only OHB caused a coupled increase in OCR and ATP synthesis, probably due to the respiratory burst that this substrate induced on OxPhos activity.

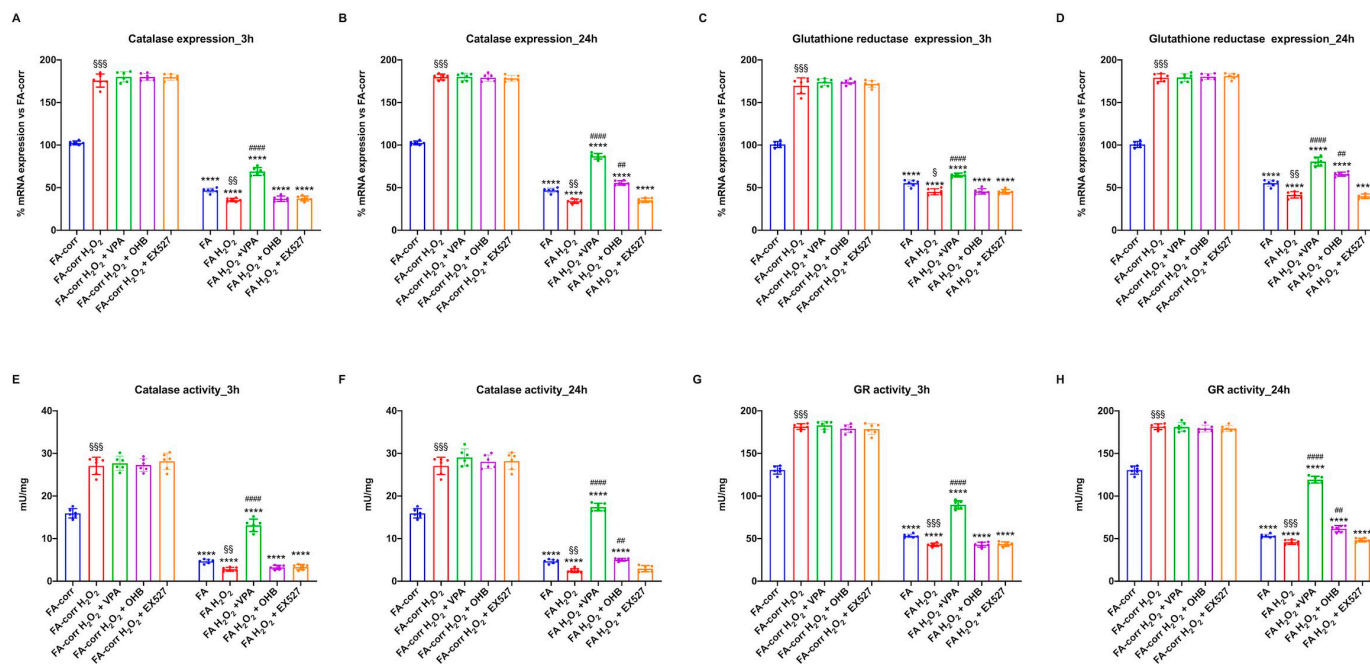


Figure 5. Modulation of catalase and glutathione reductase expression and activity in FA-corr and FA lymphoblasts treated with VPA, OHB, or EX527 after the hydrogen peroxide addition. In each graph, 0.5 mM hydrogen peroxide was added to induce oxidative insult. (A,B) Catalase (CAT) expression after 3 h and 24 h from VPA, OHB, or EX527 addition. (C,D) Glutathione reductase (GR) expression after 3 h and 24 h from VPA, OHB, or EX527 addition. (E,F) Catalase (CAT) activity after 3 h and 24 h from VPA, OHB, or EX527 addition. (G,H) Glutathione reductase (GR) activity after 3 h and 24 h from VPA, OHB, or EX527 addition. Data are reported as mean ± SD, and each graph is representative of 6 independent experiments. Statistical significance was tested with a one-way ANOVA. **** represents a significant difference for $p < 0.0001$ between FA and FA-corr cells in the same treatment condition. ## and #### represent a significant difference for $p < 0.01$ or 0.0001 , respectively, between untreated and VPA-, OHB-, or EX527-treated samples. §, §§, and §§§ represent a significant difference for $p < 0.05$, 0.01 , or 0.001 , respectively, between H₂O₂-treated and untreated samples.

In FA lymphoblasts, the H₂O₂ addition exacerbated the metabolic defects, further decreasing the electron transport between respiratory complexes I and III (Figure 6G) and the efficiency of OxPhos in the presence of both pyruvate plus malate (Figure 6A–C) and succinate (Figure 6D–F). Consequently, a reduction in cellular energy status (Figure 6H) and an increase in lipid accumulation and lipid peroxidation were observed. VPA treatment reversed all metabolic defects, causing a general recovery of OxPhos functions with an evident improvement in the coupling between OCR and ATP synthesis (Figure 6C,F), an increase in ALDH activity (Figure 6J) and the ATP/AMP ratio (Figure 6H), and a decrease in lipid content and oxidative state (Figure 6I and 6K, respectively). Conversely, OHB, due to its direct stimulating effect on the mitochondrion, induced further mitochondrial damage. In detail, OHB caused an increase in OCR but a decrease in ATP synthase, leading to further uncoupling (Figure 6A–F), associated with an increase in lipid accumulation (Figure 6I) and peroxidation (Figure 6K) and a reduction in cellular energy status (Figure 6H). EX527 exerted no effect on the H₂O₂-stressed FA lymphoblast metabolism. Similar results have been observed in primary fibroblasts (Figure S6).

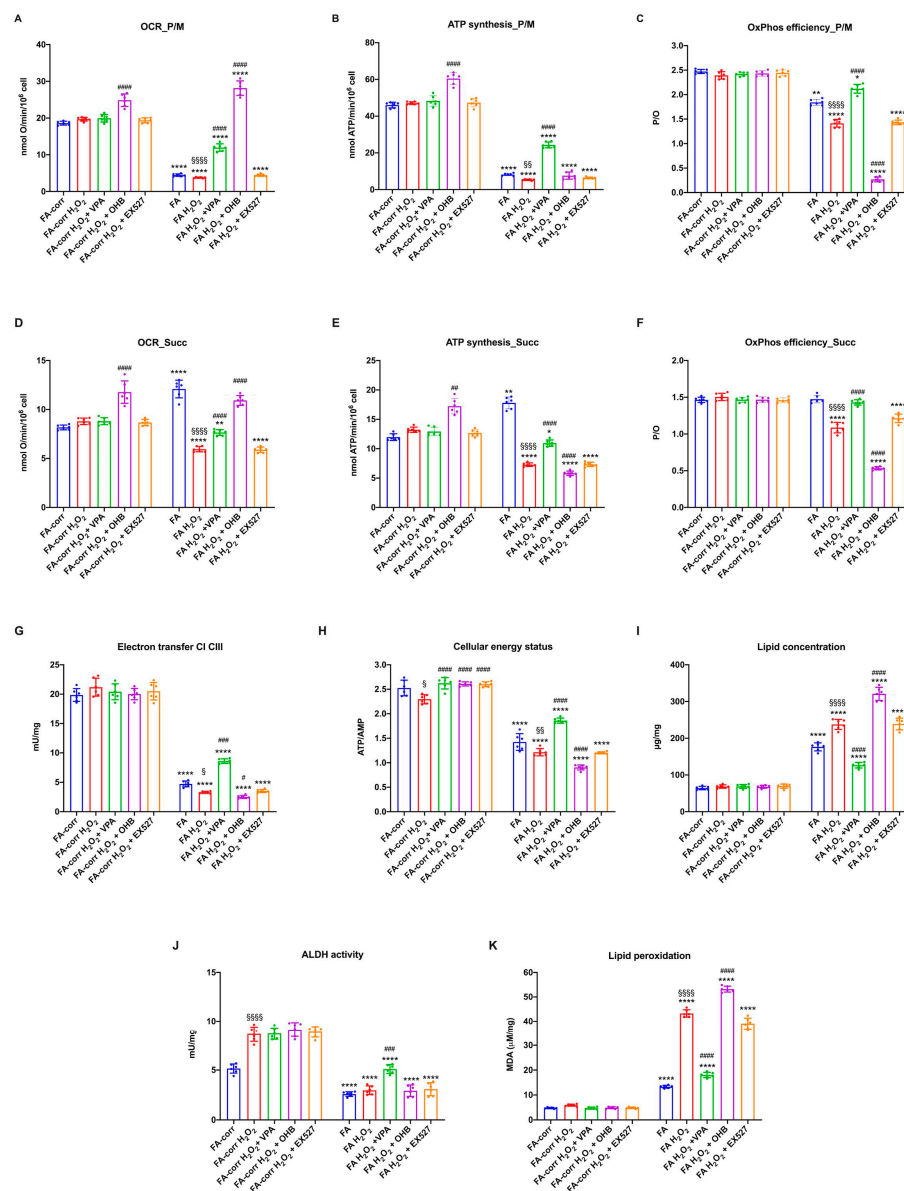


Figure 6. VPA, OHB, and EX527 effects on energy metabolism parameters and lipid peroxidation in FA-corr and FA lymphoblasts after hydrogen peroxide addition. In each graph, 0.5 mM hydrogen peroxide was added to induce oxidative damage. (A) Oxygen Consumption Rate (OCR) in the presence of pyruvate/malate (P/M). (B) ATP synthesis through F₀F₁ ATP synthase in the presence of P/M. (C) P/O ratio in the presence of P/M as an OxPhos efficiency marker. (D) Oxygen Consumption Rate (OCR) in the presence of succinate (Succ). (E) ATP synthesis through F₀F₁ ATP synthase in the presence of Succ. (F) P/O ratio in the presence of Succ as an OxPhos efficiency marker. (G) Electron transfer between complexes I and III. (H) ATP/AMP ratio as a cellular energy status marker. (I) Cellular lipid concentration. (J) Aldehyde dehydrogenase (ALDH) activity. (K) Malondialdehyde (MDA) intracellular concentration as a lipid peroxidation marker. In each panel, the effects were evaluated in lymphoblasts after 24 h from VPA, OHB, or EX527 addition. Data are reported as mean ± SD, and each graph is representative of 6 independent experiments. Statistical significance was tested opportunistically with a one-way ANOVA or two-way ANOVA. *, **, and *** represent a significant difference for *p* < 0.05, 0.01, or 0.0001, respectively, between FA and FA-corr cells in the same treatment condition. #, ##, ###, and #### represent a significant difference for *p* < 0.05, 0.01, 0.001, or 0.0001, respectively, between untreated and VPA-, OHB-, or EX527-treated samples. §, §§, and §§§§ represent a significant difference for *p* < 0.05, 0.01, or 0.0001, respectively, between H₂O₂-treated and untreated samples.

4. Discussion

Cells affected by FA are characterized by a high level of oxidative stress [16,65,66] that is not counteracted by the antioxidant defenses [8,10], as confirmed by our data on the expression and the activity of CAT and GR, two of the main ROS-detoxifying enzymes. FA cells do not also improve their own antioxidant capacity following an oxidative stimulus, such as the hydrogen peroxide addition, suggesting their inability to trigger an adaptive response to oxidative stress. On the other hand, we have already shown how FA mononuclear cells are unable to express similar levels of antioxidant activity as control cells passing from the bone marrow hypoxic environment to the normoxic environment of the bloodstream [13].

It has been suggested that this inability may depend on the hypoacetylation of gene coding for antioxidant enzymes. Therefore, in this work, lymphoblasts and fibroblasts carrying the *FANC-A* gene mutation were treated with the following deacetylase inhibitors (HDACi): VPA, OHB, and EX527 [41,43,44]. The best results were obtained after treatment with VPA, which caused an improvement in the redox state and a partial recovery of aerobic energy metabolism function. In detail, VPA induced an enhancement of CAT and GR expression and activity after three hours from treatment, maintaining the result even 24 h after adding the drug. VPA treatment also improved the extent and efficiency of OxPhos thanks to the electron transport between respiratory complex I and III recovery. This effect could depend on oxidative stress accumulation reduction, as demonstrated by the MDA level decrement since the membrane phospholipids are one of the main targets of reactive oxygen species [67]. In addition, the OxPhos efficiency is also recovered due to the UCP2 expression reduction, as the electron transport chain function depends on the inner mitochondrial membrane integrity [68]. This aerobic metabolism enhancement causes, in turn, an increase in ATP availability, both because more is produced and because the cell must consume less to restore oxidative damage. A further target of VPA also appears to be the enzyme ALDH, which is co-involved in the detoxification of aldehydes, compounds that accumulate in FA cells and favor the production of oxidative stress and DNA damage. Because of the improvement in metabolic items, VPA-treated FA cells express lower levels of DRP1 than untreated cells because it is no longer necessary to promote mitochondrial fission to isolate damaged mitochondria for elimination [69]. The reduction in DRP1 levels results in the balance recovery between fusion and fission processes, which promote mitochondrial network formation, further improving OxPhos efficiency [70].

Furthermore, the restoration of mitochondrial function due to the VPA-induced improvement of the redox state could further alter gene expression by, again, playing on acetylation levels, as a 'retrograde signaling' exists between mitochondria and the nucleus in which the impairment of mitochondrial function causes changes in the expression of some nuclear genes [71]. For example, the gene expression appears regulated by some Krebs cycle metabolites [72], whose concentration can change depending on the electron transport chain functionality. Low citrate concentrations appear to induce DNA hypoacetylation, while increased levels of 2-hydroxyglutarate, the α -ketoglutarate antagonist, would cause its hypermethylation through a decreased NAD^+/NADH ratio [73]. Thus, OxPhos function recovery could have changed the concentration of some metabolic intermediates upstream of cellular respiration, thereby modifying epigenetic signaling and the consequent gene expression. In other words, the positive loop between improved antioxidant defenses, the increased OxPhos efficiency, and mitochondrial network recovery triggered by VPA could, in turn, further modify gene expression, establishing a virtuous circle. Whatever the mechanisms by which VPA acts, at the cellular level, the result is a reduced MMC sensitivity in FA cells, suggesting less DBS accumulation. After all, Renaud et al. have already observed that another HDACi, trichostatin A, promoted DNA damage repair via homologous recombination (HR) instead of NHEJ [37]. However, it is possible to speculate that the positive effect on DNA repair depends not only on the type of mechanism used but also on a reduction in oxidative stress, aldehyde accumulation, and improved mitochondrial metabolism efficiency. In addition, to enhance the redox and energy status of FA cells

by reducing DNA damage, VPA enhances the expansion and maintenance of hematopoietic progenitors by regulating the homeobox protein HOX-4B, a transcription factor involved in HSC self-renewal [47], suggesting a possible role in maintaining the hematopoietic stem cell pool and the aplasia risk reduction.

However, not all HDACi tested positively affected the redox balance and energy metabolism of FA cells. Treatment with OHB had opposite effects to those observed with VPA, although both molecules belong to HDACi classes I and II. In detail, OHB did not cause a decrease in oxidative damage, despite the slight increase in CAT and GR expression and the electron transfer between complexes I and III only after 24 h from the treatment. In contrast, OHB promoted further uncoupling of OxPhos and an accumulation of lipids and malondialdehyde. This opposite effect to VPA could be explained by the fact that OHB causes a respiratory burst that forces OxPhos activity, exacerbating the metabolic defect and increasing oxidative stress production. In addition, the unfunctional mitochondrial metabolism exacerbates the lipid accumulation in the cell, probably due to the increased AcetylCoA level [15], incrementing the risk of lipid peroxidation. These data suggest that metabolic and oxidative damages in FA cells depend on several factors, which should be corrected simultaneously to ensure a complete recovery of cell function. The opposite effects of VPA and OHB were observed even more after treatment with hydrogen peroxide, since whereas VPA induces, as in the case of basal conditions, an improvement in redox and biochemical parameters, OHB causes a further impairment of mitochondrial functions and an increase in oxidative stress.

EX527, a class III HDACi, does not display effects on FA cells, suggesting that, in FA cells, sirt1 does not play a pivotal role in aerobic metabolism regulation.

5. Conclusions

The data reported in this paper suggest that the *FANCA* gene may be involved in determining DNA acetylation levels. Furthermore, VPA appears to have promising effects in improving the redox and metabolic aspect of FA cells, emphasizing, once again, that the accumulation of oxidative stress and altered energy metabolism play a strategic role in this pathology beyond the defect in DNA repair.

Supplementary Materials: The following supporting information can be downloaded at <https://www.mdpi.com/article/10.3390/antiox12051100/s1>. Figure S1: Comparison of biochemical activities in the healthy donor-derived and FA-corr lymphoblast cell lines; Figure S2: Comparison of biochemical activities in the healthy donor-derived and FA-corr primary fibroblasts; Figure S3: Modulation of Catalase and Glutathione Reductase expression and activity in FA fibroblasts treated with VPA, OHB, or EX527; Figure S4: VPA, OHB, and EX527 effects on energy metabolism parameters and lipid peroxidation in FA fibroblasts; Figure S5: Modulation of Catalase and Glutathione Reductase expression and activity in FA fibroblasts treated with VPA, OHB, or EX527 after the hydrogen peroxide addition; Figure S6: VPA, OHB, and EX527 effects on energy metabolism parameters and lipid peroxidation in FA fibroblasts after the hydrogen peroxide addition.

Author Contributions: Conceptualization, E.C. and S.R. (Silvia Ravera); methodology, S.R. (Silvia Ravera); validation, S.B., E.C. and S.R. (Silvia Ravera); formal analysis, S.R. (Silvia Ravera); investigation, N.B., S.R. (Stefano Regis), S.B., A.N.M., F.S., S.R. (Silvia Ravera) and E.C.; resources, M.S., M.L., F.C. and E.C.; data curation, S.R. (Silvia Ravera); writing—original draft preparation, E.C. and S.R. (Silvia Ravera); writing—review and editing, E.C. and S.R. (Silvia Ravera); visualization, S.R. (Silvia Ravera); supervision, E.C. and S.R. (Silvia Ravera); project administration, S.R. (Silvia Ravera); funding acquisition, E.C. and S.R. (Silvia Ravera). All authors have read and agreed to the published version of the manuscript.

Funding: This research was funded by AIRFA—Associazione Italiana Ricerca su Anemia di Fanconi (Grant number: #AIRFA2019). ANM received funding from the European Union Horizon 2020 research and innovation program under the Marie Skłodowska-Curie grant agreement No. 101023721.

Institutional Review Board Statement: This study was in accordance with the precepts established by the Helsinki Declaration. The samples were obtained from the ‘Cell Line and DNA Biobank from Patients affected by Genetic Diseases’ (G. Gaslini Institute) e Telethon Genetic Biobank Network (project no. GTB07001).

Informed Consent Statement: Not applicable.

Data Availability Statement: All of the data is contained within the article and the Supplementary Materials.

Acknowledgments: We want to acknowledge ERG SpA, Cambiaso and Risso, Rimorchiatori Riuniti, and Saar Depositi Oleari Portuali for supporting the activity of the Clinical and Experimental Hematology Unit of the G. Gaslini Institute.

Conflicts of Interest: The authors declare no conflict of interest.

References

- De Winter, J.P.; Joenje, H. The Genetic and Molecular Basis of Fanconi Anemia. *Mutat. Res.* **2009**, *668*, 11–19. [[CrossRef](#)] [[PubMed](#)]
- Castella, M.; Pujol, R.; Callén, E.; Trujillo, J.P.; Casado, J.A.; Gille, H.; Lach, F.P.; Auerbach, A.D.; Schindler, D.; Benítez, J.; et al. Origin, Functional Role, and Clinical Impact of Fanconi Anemia FANCA Mutations. *Blood* **2011**, *117*, 3759–3769. [[CrossRef](#)] [[PubMed](#)]
- Marsit, C.J.; Liu, M.; Nelson, H.H.; Posner, M.; Suzuki, M.; Kelsey, K.T. Inactivation of the Fanconi Anemia/BRCA Pathway in Lung and Oral Cancers: Implications for Treatment and Survival. *Oncogene* **2004**, *23*, 1000–1004. [[CrossRef](#)] [[PubMed](#)]
- Cappelli, E.; Degan, P.; Dufour, C.; Ravera, S. Aerobic Metabolism Dysfunction as One of the Links between Fanconi Anemia-Deficient Pathway and the Aggressive Cell Invasion in Head and Neck Cancer Cells. *Oral Oncol.* **2018**, *87*, 210–211. [[CrossRef](#)]
- Del Valle, J.; Rofes, P.; Moreno-Cabrera, J.M.; López-Dóriga, A.; Belhadj, S.; Vargas-Parra, G.; Teulé, À.; Cuesta, R.; Muñoz, X.; Campos, O.; et al. Exploring the Role of Mutations in Fanconi Anemia Genes in Hereditary Cancer Patients. *Cancers* **2020**, *12*, 829. [[CrossRef](#)] [[PubMed](#)]
- García-De-teresa, B.; Rodríguez, A.; Frias, S. Chromosome Instability in Fanconi Anemia: From Breaks to Phenotypic Consequences. *Genes* **2020**, *11*, 1528. [[CrossRef](#)]
- Grompe, M.; D’Andrea, A. Fanconi Anemia and DNA Repair. *Hum. Mol. Genet.* **2001**, *10*, 2253–2259. [[CrossRef](#)]
- Lyakhovich, A. Damaged Mitochondria and Overproduction of ROS in Fanconi Anemia Cells. *Rare Dis.* **2013**, *1*, e24048. [[CrossRef](#)]
- Pagano, G.; Talamanca, A.A.; Castello, G.; d’Ischia, M.; Pallardó, F.V.; Petrović, S.; Porto, B.; Tiano, L.; Zatterale, A. From Clinical Description, to in Vitro and Animal Studies, and Backward to Patients: Oxidative Stress and Mitochondrial Dysfunction in Fanconi Anemia. *Free Radic. Biol. Med.* **2013**, *58*, 118–125. [[CrossRef](#)]
- Kumari, U.; Ya Jun, W.; Huat Bay, B.; Lyakhovich, A. Evidence of Mitochondrial Dysfunction and Impaired ROS Detoxifying Machinery in Fanconi Anemia Cells. *Oncogene* **2014**, *33*, 165–172. [[CrossRef](#)]
- Cappelli, E.; Ravera, S.; Vaccaro, D.; Cuccarolo, P.; Bartolucci, M.; Panfoli, I.; Dufour, C.; Degan, P. Mitochondrial Respiratory Complex I Defects in Fanconi Anemia. *Trends Mol. Med.* **2013**, *19*, 513–514. [[CrossRef](#)] [[PubMed](#)]
- Ravera, S.; Vaccaro, D.; Cuccarolo, P.; Columbaro, M.; Capanni, C.; Bartolucci, M.; Panfoli, I.; Morelli, A.; Dufour, C.; Cappelli, E.; et al. Mitochondrial Respiratory Chain Complex i Defects in Fanconi Anemia Complementation Group A. *Biochimie* **2013**, *95*, 1828–1837. [[CrossRef](#)] [[PubMed](#)]
- Cappelli, E.; Degan, P.; Bruno, S.; Pierri, F.; Miano, M.; Raggi, F.; Farruggia, P.; Mecucci, C.; Crescenzi, B.; Naim, V.; et al. The Passage from Bone Marrow Niche to Bloodstream Triggers the Metabolic Impairment in Fanconi Anemia Mononuclear Cells. *Redox Biol.* **2020**, *36*, 101618. [[CrossRef](#)]
- Cappelli, E.; Cuccarolo, P.; Stroppiana, G.; Miano, M.; Bottega, R.; Cossu, V.; Degan, P.; Ravera, S. Defects in Mitochondrial Energetic Function Compels Fanconi Anaemia Cells to Glycolytic Metabolism. *Biochim. Biophys. Acta Mol. Basis Dis.* **2017**, *1863*, 1214–1221. [[CrossRef](#)] [[PubMed](#)]
- Ravera, S.; Degan, P.; Sabatini, F.; Columbaro, M.; Dufour, C.; Cappelli, E. Altered Lipid Metabolism Could Drive the Bone Marrow Failure in Fanconi Anaemia. *Br. J. Haematol.* **2019**, *184*, 693–696. [[CrossRef](#)]
- Du, W.; Adam, Z.; Rani, R.; Zhang, X.; Pang, Q. Oxidative Stress in Fanconi Anemia Hematopoiesis and Disease Progression. *Antioxid. Redox Signal.* **2008**, *10*, 1909–1921. [[CrossRef](#)] [[PubMed](#)]
- Cappelli, E.; Bertola, N.; Bruno, S.; Degan, P.; Regis, S.; Corsolini, F.; Banelli, B.; Dufour, C.; Ravera, S. A Multidrug Approach to Modulate the Mitochondrial Metabolism Impairment and Relative Oxidative Stress in Fanconi Anemia Complementation Group A. *Metabolites* **2021**, *12*, 6. [[CrossRef](#)]
- Wang, D.; Chen, Y.M.; Ruan, M.H.; Zhou, A.H.; Qian, Y.; Chen, C. Homocysteine Inhibits Neural Stem Cells Survival by Inducing DNA Interstrand Cross-Links via Oxidative Stress. *Neurosci. Lett.* **2016**, *635*, 24–32. [[CrossRef](#)]
- Jura, J.; Węgrzyn, P.; Jura, J.; Koj, A. Regulatory Mechanisms of Gene Expression: Complexity with Elements of Deterministic Chaos. *Acta Biochim. Polonica* **2006**, *53*, 1–9. [[CrossRef](#)]
- Verdone, L.; Caserta, M.; di Mauro, E. Role of Histone Acetylation in the Control of Gene Expression. *Biochem. Cell Biol.* **2005**, *83*, 344–353. [[CrossRef](#)]

21. Peserico, A.; Simone, C. Physical and Functional HAT/HDAC Interplay Regulates Protein Acetylation Balance. *J. Biomed. Biotechnol.* **2011**, *2011*, 371832. [[CrossRef](#)] [[PubMed](#)]
22. Drazic, A.; Myklebust, L.M.; Ree, R.; Arnesen, T. The World of Protein Acetylation. *Biochim. Biophys. Acta BBA Proteins Proteomics* **2016**, *1864*, 1372–1401. [[CrossRef](#)]
23. Park, S.Y.; Kim, J.S. A Short Guide to Histone Deacetylases Including Recent Progress on Class II Enzymes. *Exp. Mol. Med.* **2020**, *52*, 204–212. [[CrossRef](#)] [[PubMed](#)]
24. Chen, H.P.; Zhao, Y.T.; Zhao, T.C. Histone Deacetylases and Mechanisms of Regulation of Gene Expression (Histone Deacetylases in Cancer). *Crit. Rev. Oncog.* **2015**, *20*, 35. [[CrossRef](#)] [[PubMed](#)]
25. Dokmanovic, M.; Clarke, C.; Marks, P.A. Histone Deacetylase Inhibitors: Overview and Perspectives. *Mol. Cancer Res.* **2007**, *5*, 981–989. [[CrossRef](#)]
26. Adcock, I.M. HDAC Inhibitors as Anti-Inflammatory Agents. *Br. J. Pharmacol.* **2007**, *150*, 829. [[CrossRef](#)]
27. Ran, J.; Zhou, J. Targeted Inhibition of Histone Deacetylase 6 in Inflammatory Diseases. *Thorac. Cancer* **2019**, *10*, 405. [[CrossRef](#)]
28. Nijhuis, L.; Peeters, J.G.C.; Vastert, S.J.; van Loosdregt, J. Restoring T Cell Tolerance, Exploring the Potential of Histone Deacetylase Inhibitors for the Treatment of Juvenile Idiopathic Arthritis. *Front. Immunol.* **2019**, *10*, 151. [[CrossRef](#)]
29. Grabiec, A.M.; Krausz, S.; de Jager, W.; Burakowski, T.; Groot, D.; Sanders, M.E.; Prakken, B.J.; Maslinski, W.; Eldering, E.; Tak, P.P.; et al. Histone Deacetylase Inhibitors Suppress Inflammatory Activation of Rheumatoid Arthritis Patient Synovial Macrophages and Tissue. *J. Immunol.* **2010**, *184*, 2718–2728. [[CrossRef](#)]
30. Ke, X.; Lin, Z.; Ye, Z.; Leng, M.; Chen, B.; Jiang, C.; Jiang, X.; Li, G. Histone Deacetylases in the Pathogenesis of Diabetic Cardiomyopathy. *Front. Endocrinol.* **2021**, *12*, 679655. [[CrossRef](#)]
31. Li, G.; Tian, Y.; Zhu, W.G. The Roles of Histone Deacetylases and Their Inhibitors in Cancer Therapy. *Front. Cell Dev. Biol.* **2020**, *8*, 1004. [[CrossRef](#)] [[PubMed](#)]
32. Adams, C.M.; Eischen, C.M. Histone Deacetylase Inhibition Reveals a Tumor-Suppressive Function of MYC-Regulated MiRNA in Breast and Lung Carcinoma. *Cell Death Differ.* **2016**, *23*, 1312–1321. [[CrossRef](#)] [[PubMed](#)]
33. Sun, X.J.; Man, N.; Tan, Y.; Nimer, S.D.; Wang, L. The Role of Histone Acetyltransferases in Normal and Malignant Hematopoiesis. *Front. Oncol.* **2015**, *5*, 108. [[CrossRef](#)]
34. Becherini, P.; Caffa, I.; Piacente, F.; Damonte, P.; Vellone, V.G.; Passalacqua, M.; Benzi, A.; Bonfiglio, T.; Reverberi, D.; Khalifa, A.; et al. SIRT6 Enhances Oxidative Phosphorylation in Breast Cancer and Promotes Mammary Tumorigenesis in Mice. *Cancer Metab.* **2021**, *9*, 6. [[CrossRef](#)]
35. Falkenberg, K.J.; Johnstone, R.W. Histone Deacetylases and Their Inhibitors in Cancer, Neurological Diseases and Immune Disorders. *Nat. Rev. Drug Discov.* **2014**, *13*, 673–691. [[CrossRef](#)] [[PubMed](#)]
36. Shukla, S.; Tekwani, B.L. Histone Deacetylases Inhibitors in Neurodegenerative Diseases, Neuroprotection and Neuronal Differentiation. *Front. Pharmacol.* **2020**, *11*, 537. [[CrossRef](#)]
37. Renaud, E.; Barascu, A.; Rosselli, F. Impaired TIP60-Mediated H4K16 Acetylation Accounts for the Aberrant Chromatin Accumulation of 53BP1 and RAP80 in Fanconi Anemia Pathway-Deficient Cells. *Nucleic Acids Res.* **2016**, *44*, 648–656. [[CrossRef](#)] [[PubMed](#)]
38. Roos, W.P.; Krumm, A. The Multifaceted Influence of Histone Deacetylases on DNA Damage Signalling and DNA Repair. *Nucleic Acids Res.* **2016**, *44*, 10017. [[CrossRef](#)]
39. Robert, C.; Nagaria, P.K.; Pawar, N.; Adewuyi, A.; Gojo, I.; Meyers, D.J.; Cole, P.A.; Rassool, F.V. Histone Deacetylase Inhibitors Decrease NHEJ Both by Acetylation of Repair Factors and Trapping of PARP1 at DNA Double-Strand Breaks in Chromatin. *Leuk. Res.* **2016**, *45*, 14–23. [[CrossRef](#)]
40. Löscher, W. Basic Pharmacology of Valproate: A Review after 35 Years of Clinical Use for the Treatment of Epilepsy. *CNS Drugs* **2002**, *16*, 669–694. [[CrossRef](#)]
41. Gurvich, N.; Tsygankova, O.M.; Meinkoth, J.L.; Klein, P.S. Histone Deacetylase Is a Target of Valproic Acid-Mediated Cellular Differentiation. *Cancer Res.* **2004**, *64*, 1079–1086. [[CrossRef](#)] [[PubMed](#)]
42. Bolden, J.E.; Peart, M.J.; Johnstone, R.W. Anticancer Activities of Histone Deacetylase Inhibitors. *Nat. Rev. Drug Disc.* **2006**, *5*, 769–784. [[CrossRef](#)] [[PubMed](#)]
43. Shimazu, T.; Hirschey, M.D.; Newman, J.; He, W.; Shirakawa, K.; Le Moan, N.; Grueter, C.A.; Lim, H.; Saunders, L.R.; Stevens, R.D.; et al. Suppression of Oxidative Stress by β -Hydroxybutyrate, an Endogenous Histone Deacetylase Inhibitor. *Science* **2013**, *339*, 211. [[CrossRef](#)]
44. Broussy, S.; Laaroussi, H.; Vidal, M. Biochemical Mechanism and Biological Effects of the Inhibition of Silent Information Regulator 1 (SIRT1) by EX527 (SEN0014196 or Selisistat). *J. Enzym. Inhib. Med. Chem.* **2020**, *35*, 1124. [[CrossRef](#)]
45. Rifai, K.; Judes, G.; Idrissou, M.; Dures, M.; Bignon, Y.J.; Penault-Llorca, F.; Bernard-Gallon, D. SIRT1-Dependent Epigenetic Regulation of H3 and H4 Histone Acetylation in Human Breast Cancer. *Oncotarget* **2018**, *9*, 30661. [[CrossRef](#)] [[PubMed](#)]
46. Verdin, E.; Hirschey, M.D.; Finley, L.W.S.; Haigis, M.C. Sirtuin Regulation of Mitochondria: Energy Production, Apoptosis, and Signaling. *Trends Biochem. Sci.* **2010**, *35*, 669–675. [[CrossRef](#)] [[PubMed](#)]
47. De Felice, L.; Tatarelli, C.; Mascolo, M.G.; Gregorj, C.; Agostini, F.; Fiorini, R.; Gelmetti, V.; Pascale, S.; Padula, F.; Petrucci, M.T.; et al. Histone Deacetylase Inhibitor Valproic Acid Enhances the Cytokine-Induced Expansion of Human Hematopoietic Stem Cells. *Cancer Res.* **2005**, *65*, 1505–1513. [[CrossRef](#)]

48. Mikami, D.; Kobayashi, M.; Uwada, J.; Yazawa, T.; Kamiyama, K.; Nishimori, K.; Nishikawa, Y.; Nishikawa, S.; Yokoi, S.; Taniguchi, T.; et al. β -Hydroxybutyrate Enhances the Cytotoxic Effect of Cisplatin via the Inhibition of HDAC/Survivin Axis in Human Hepatocellular Carcinoma Cells. *J. Pharmacol. Sci.* **2020**, *142*, 1–8. [[CrossRef](#)]
49. Hanenberg, H.; Pollok, K.E.; Vieten, L.; Verlander, P.C.; Leurs, C.; Cooper, R.J.; Göttische, K.; Haneline, L.; Clapp, D.W.; Lobitz, S.; et al. Phenotypic Correction of Primary Fanconi Anemia T Cells with Retroviral Vectors as a Diagnostic Tool. *Exp. Hematol.* **2002**, *30*, 410–420. [[CrossRef](#)]
50. Bradford, M.M. A Rapid and Sensitive Method for the Quantitation of Microgram Quantities of Protein Utilizing the Principle of Protein-Dye Binding. *Anal. Biochem.* **1976**, *72*, 248–254. [[CrossRef](#)]
51. Bianchi, G.; Ravera, S.; Traverso, C.; Amaro, A.; Piaggio, F.; Emionite, L.; Bachetti, T.; Pfeffer, U.; Raffaghello, L. Curcumin Induces a Fatal Energetic Impairment in Tumor Cells in Vitro and in Vivo by Inhibiting ATP-Synthase Activity. *Carcinogenesis* **2018**, *39*, 1141–1150. [[CrossRef](#)]
52. Bertola, N.; Degan, P.; Cappelli, E.; Ravera, S. Mutated FANCA Gene Role in the Modulation of Energy Metabolism and Mitochondrial Dynamics in Head and Neck Squamous Cell Carcinoma. *Cells* **2022**, *11*, 2353. [[CrossRef](#)] [[PubMed](#)]
53. Solito, R.; Corti, F.; Chen, C.H.; Mochly-Rosen, D.; Giachetti, A.; Ziche, M.; Donnini, S. Mitochondrial Aldehyde Dehydrogenase-2 Activation Prevents β -Amyloid-Induced Endothelial Cell Dysfunction and Restores Angiogenesis. *J. Cell Sci.* **2013**, *126*, 1952–1961. [[CrossRef](#)] [[PubMed](#)]
54. Colla, R.; Izzotti, A.; de Ciucis, C.; Fenoglio, D.; Ravera, S.; Speciale, A.; Ricciarelli, R.; Furfaro, A.L.; Pulliero, A.; Passalacqua, M.; et al. Glutathione-Mediated Antioxidant Response and Aerobic Metabolism: Two Crucial Factors Involved in Determining the Multi-Drug Resistance of High-Risk Neuroblastoma. *Oncotarget* **2016**, *7*, 70715. [[CrossRef](#)]
55. Amaroli, A.; Pasquale, C.; Zekiy, A.; Utyuzh, A.; Benedicenti, S.; Signore, A.; Ravera, S. Photobiomodulation and Oxidative Stress: 980 Nm Diode Laser Light Regulates Mitochondrial Activity and Reactive Oxygen Species Production. *Oxid. Med. Cell Longev.* **2021**, *2021*, 1–11. [[CrossRef](#)]
56. Ravera, S.; Dufour, C.; Cesaro, S.; Bottega, R.; Faleschini, M.; Cuccarolo, P.; Corsolini, F.; Usai, C.; Columbaro, M.; Cipolli, M.; et al. Evaluation of Energy Metabolism and Calcium Homeostasis in Cells Affected by Shwachman-Diamond Syndrome. *Sci. Rep.* **2016**, *6*, 25441. [[CrossRef](#)] [[PubMed](#)]
57. Ravera, S.; Ghiotto, F.; Tenca, C.; Gugliatti, E.; Santamaria, S.; Ledda, B.; Ibatci, A.; Cutrona, G.; Mazzarello, A.N.; Bagnara, D.; et al. Berberine Affects Mitochondrial Activity and Cell Growth of Leukemic Cells from Chronic Lymphocytic Leukemia Patients. *Sci. Rep.* **2020**, *10*, 16519. [[CrossRef](#)]
58. Hinkle, P.C. P/O Ratios of Mitochondrial Oxidative Phosphorylation. *Biochim. Biophys. Acta* **2005**, *1706*, 1–11. [[CrossRef](#)]
59. López-Doménech, G.; Covill-Cooke, C.; Ivankovic, D.; Halff, E.F.; Sheehan, D.F.; Norkett, R.; Birsa, N.; Kittler, J.T. Miro Proteins Coordinate Microtubule- and Actin-Dependent Mitochondrial Transport and Distribution. *EMBO J.* **2018**, *37*, 321–336. [[CrossRef](#)]
60. Bottega, R.; Napolitano, L.M.R.; Carbone, A.; Cappelli, E.; Corsolini, F.; Onesti, S.; Savoia, A.; Gasparini, P.; Faletra, F. Two Further Patients with Warsaw Breakage Syndrome. Is a Mild Phenotype Possible? *Mol. Genet. Genomic Med.* **2019**, *7*, e639. [[CrossRef](#)]
61. Ravera, S.; Dufour, C.; Degan, P.; Cappelli, E. Fanconi Anemia: From DNA Repair to Metabolism. *Eur. J. Hum. Genet.* **2018**, *26*, 475–476. [[CrossRef](#)]
62. Degan, P.; Cappelli, E.; Regis, S.; Ravera, S. New Insights and Perspectives in Fanconi Anemia Research. *Trends Mol. Med.* **2019**, *25*, 167–170. [[CrossRef](#)] [[PubMed](#)]
63. Bertola, N.; Bruno, S.; Capanni, C.; Columbaro, M.; Mazzarello, A.N.; Corsolini, F.; Regis, S.; Degan, P.; Cappelli, E.; Ravera, S. Altered Mitochondrial Dynamic in Lymphoblasts and Fibroblasts Mutated for FANCA-A Gene: The Central Role of DRP1. *Int. J. Mol. Sci.* **2023**, *24*, 6557. [[CrossRef](#)] [[PubMed](#)]
64. Columbaro, M.; Ravera, S.; Capanni, C.; Panfoli, I.; Cuccarolo, P.; Stroppiana, G.; Degan, P.; Cappelli, E. Treatment of FANCA Cells with Resveratrol and N-Acetylcysteine: A Comparative Study. *PLoS ONE* **2014**, *9*, e104857. [[CrossRef](#)] [[PubMed](#)]
65. Pagano, G.; Degan, P.; D'Ischia, M.; Kelly, F.J.; Nobili, B.; Pallardó, F.V.; Youssoufian, H.; Zatterale, A. Oxidative Stress as a Multiple Effector in Fanconi Anaemia Clinical Phenotype. *Eur. J. Haematol.* **2005**, *75*, 93–100. [[CrossRef](#)] [[PubMed](#)]
66. El-Bassyouni, H.T.; Afifi, H.H.; Eid, M.M.; Kamal, R.M.; El-Gebali, H.H.; El-Saeed, G.; Thomas, M.M.; Abdel-Maksoud, S.A. Oxidative Stress—a Phenotypic Hallmark of Fanconi Anemia and Down Syndrome: The Effect of Antioxidants. *Ann. Med. Health Sci. Res.* **2015**, *5*, 205. [[CrossRef](#)]
67. Juan, C.A.; de la Lastra, J.M.P.; Plou, F.J.; Pérez-Lebeña, E. The Chemistry of Reactive Oxygen Species (ROS) Revisited: Outlining Their Role in Biological Macromolecules (DNA, Lipids and Proteins) and Induced Pathologies. *Int. J. Mol. Sci.* **2021**, *22*, 4642. [[CrossRef](#)]
68. Hroudová, J.; Fišar, Z. Control Mechanisms in Mitochondrial Oxidative Phosphorylation. *Neural. Regen. Res.* **2013**, *8*, 363–375. [[CrossRef](#)]
69. Wai, T.; Langer, T. Mitochondrial Dynamics and Metabolic Regulation. *Trends Endocrinol. Metab.* **2016**, *27*, 105–117. [[CrossRef](#)]
70. Ravera, S.; Podestà, M.; Sabatini, F.; Fresia, C.; Columbaro, M.; Bruno, S.; Fulcheri, E.; Ramenghi, L.A.; Frassoni, F. Mesenchymal Stem Cells from Preterm to Term Newborns Undergo a Significant Switch from Anaerobic Glycolysis to the Oxidative Phosphorylation. *Cell Mol. Life Sci.* **2018**, *75*, 889–903. [[CrossRef](#)]
71. Yang, D.; Kim, J. Mitochondrial Retrograde Signalling and Metabolic Alterations in the Tumour Microenvironment. *Cells* **2019**, *8*, 275. [[CrossRef](#)] [[PubMed](#)]

72. Li, W.; Long, Q.; Wu, H.; Zhou, Y.; Duan, L.; Yuan, H.; Ding, Y.; Huang, Y.; Wu, Y.; Huang, J.; et al. Nuclear Localization of Mitochondrial TCA Cycle Enzymes Modulates Pluripotency via Histone Acetylation. *Nat. Commun.* **2022**, *13*, 1–15. [[CrossRef](#)] [[PubMed](#)]
73. Ansó, E.; Weinberg, S.E.; Diebold, L.P.; Thompson, B.J.; Malinge, S.; Schumacker, P.T.; Liu, X.; Zhang, Y.; Shao, Z.; Steadman, M.; et al. The Mitochondrial Respiratory Chain Is Essential for Haematopoietic Stem Cell Function. *Nat. Cell Biol.* **2017**, *19*, 614–625. [[CrossRef](#)] [[PubMed](#)]

Disclaimer/Publisher’s Note: The statements, opinions and data contained in all publications are solely those of the individual author(s) and contributor(s) and not of MDPI and/or the editor(s). MDPI and/or the editor(s) disclaim responsibility for any injury to people or property resulting from any ideas, methods, instructions or products referred to in the content.